

This document is confidential and is proprietary to the American Chemical Society and its authors. Do not copy or disclose without written permission. If you have received this item in error, notify the sender and delete all copies.

A pH-induced switch in GLP-1 aggregation kinetics

| | |
|-------------------------------|---|
| Journal: | <i>Journal of the American Chemical Society</i> |
| Manuscript ID | ja-2016-05025f.R1 |
| Manuscript Type: | Article |
| Date Submitted by the Author: | n/a |
| Complete List of Authors: | Zapadka, Karolina; University of Cambridge, Chemistry Becher, Frederik; University of Cambridge, Chemistry Uddin, Shahid; MedImmune Ltd, Formulaton Science Varley, Paul; MedImmune Ltd Bishop, Steven; MedImmune, Process Biochemistry and Formulation Sciences Gomes dos Santos, Ana; MedImmune Ltd, Formulaton Science Jackson, Sophie; University of Cambridge, Chemistry |
| | |

SCHOLARONE™
Manuscripts

A pH-induced switch in GLP-1 aggregation kinetics

Karolina L. Zapadka[†], Frederik J. Becher[†], Shahid Uddin[‡], Paul G. Varley[‡], Steve Bishop[‡], A. L. Gomes dos Santos[‡] & Sophie E. Jackson^{†*}

[†]Department of Chemistry, University of Cambridge, Cambridge, CB2 1EW, U.K.

[‡]Formulation Sciences, MedImmune Ltd., Granta Park, Cambridge, CB21 6GH, U.K.

[‡]Formulation Sciences, One MedImmune Way, Gaithersburg, MD 20878, U.S.A.

KEYWORDS aggregation, amyloid formation, off-pathway oligomers, GLP-1, ThT assay

ABSTRACT: Aggregation and amyloid fibril formation of peptides and proteins is a widespread phenomenon. It has serious implications in a range of areas from biotechnological and pharmaceutical applications to medical disorders. The aim of this study was to develop a better understanding of the mechanism of aggregation and amyloid fibrillation of an important pharmaceutical GLP-1. GLP-1 is a 31-residue hormone peptide that plays an important role regulating blood glucose levels, analogues of which are used for treatment of type 2 diabetes. Amyloid fibril formation of GLP-1 was monitored using thioflavin T fluorescence as a function of peptide concentration between 7.5 – 8.2. Results from these studies establish that there is a highly unusual pH-induced switch in GLP-1 aggregation kinetics. At pH 8.2, the kinetics are consistent with a nucleation-polymerization mechanism for fibril formation. However, at pH 7.5, highly unusual kinetics are observed, where the lag time increases with increasing peptide concentration. We attribute this result to the formation of off-pathway species together with an initial slow, unimolecular step where monomer converts to a different monomeric form that forms on-pathway oligomers and ultimately fibrils. Estimation of the pK_a values of all the ionisable groups in GLP-1 suggest it is the protonation/deprotonation of the N-terminus that is responsible for the switch with pH. In addition, a range of biophysical techniques were used to characterize 1) the start point of the aggregation reaction and 2) the structure and stability of the fibrils formed. These results show that the off-pathway species form under conditions where GLP-1 is most prone to form oligomers.

INTRODUCTION

The aggregation of peptides and proteins into β -sheet rich amyloid fibrils is a common process increasingly associated with problems in drug development and pharmaceutical applications, as well as many disease states.¹ Although significant progress has been made over the past 15 years in elucidating the structure² and morphology³ of amyloid fibrils and their mechanism of formation⁴⁻⁵, our current understanding of how peptides and proteins aggregate into fibrils remains incomplete. It has been shown that amyloid fibrils are commonly formed through a nucleation-polymerization (N-P) mechanism with characteristic sigmoidal-like kinetics. There is an initial lag phase, during which critical nucleating species are formed, which is followed by a rapid growth phase, and then a plateau as the system either reaches equilibrium or the monomer levels are completely depleted.⁶⁻⁵

Oligomers have often been observed to form during fibril formation, albeit at sometimes very low concentrations⁷⁻⁸. However, many aspects of the relationship between oligomers and the mechanism of fibril formation are not yet fully understood.⁸ Considerable progress has been made in understanding some of the factors affecting the aggregation propensity of a system which has been shown to depend upon sequence, monomer conformation, nucleation rate, effective monomer concentration, pH, ionic strength, small molecules and external factors such as temperature or agitation.^{5,9-10}

In this work, we focus on the human glucagon-like peptide-1, GLP-1 (7-37), which is a 31-residue hormone peptide.¹¹ GLP-1 plays an important role in our body regulating blood glucose levels through regulation of glucose-dependent insulin secretion, inhibition of glucagon secretion and gastric emptying together with reduction of food intake.¹¹ It is an important pharmaceutical molecule, analogues of which are used for the treatment of type 2 diabetes.¹¹⁻¹² It has previously been reported that GLP-1 aggregates into amyloid fibrils under physiological conditions¹³ and at pH 5.8.¹⁴

Here, we present the results of a detailed study of the pH dependence of the aggregation kinetics of GLP-1. Aggregation kinetics were monitored by thioflavin T (ThT) which increases its fluorescence upon binding to β -sheet rich amyloid fibrils.⁵ Kinetic data from these experiments were analysed to obtain the apparent growth rate, $t_{1/2}$ and lag time at different peptide concentrations and pH values. We report an unusual pH-induced switch in GLP-1 aggregation kinetics.

In order to understand the complex, pH-dependent aggregation kinetics obtained, a detailed characterization of freshly prepared samples of GLP-1 was undertaken using a range of biophysical techniques to obtain information on the size, structure, and oligomeric state of species present. This included analytical ultracentrifugation (AUC), asymmetric flow field-flow fractionation (AF4) with multi-angle light scattering detector (MALS), dynamic light scattering (DLS), size-exclusion chromatography (SEC), far-UV circular dichroism (far-UV CD) and ANS-binding assays. In all cases, fibrils formed

1 were confirmed using atomic force microscopy (AFM) and
2 transmission electron microscopy (TEM) providing infor-
3 mation on the structure, stability and morphology of the fibrils
4 and how this depends upon pH.

5 EXPERIMENTAL SECTION

6 **Materials.** The 31-residue GLP-1 (7-37)
7 (HAEGTFTSDVSSYLEGQAAKEFIAWLVKGRG) was pur-
8 chased from Bachem (98.5% pure), with a molecular weight
9 of 3.36 kDa and used without further purification. GLP-1
10 powder was dissolved in buffer (25 mM sodium phosphate at
11 pH 7.5 or 25 mM Tris-HCl at pH 8.0 or 8.5) to a final concen-
12 tration of 298 μM . The solution was filtered (0.22 μm filter)
13 prior to use, and the concentration was determined spectro-
14 photometrically using a NanoDrop spectrophotometer (ND
15 2000, Thermo Scientific), and a theoretical extinction coeffi-
16 cient of 6990 $\text{M}^{-1}\text{cm}^{-1}$ at 280 nm. All other chemicals were of
17 analytical grade.

18 **Kinetics of aggregation: Thioflavin T binding assays.** For
19 kinetic experiments, a stock solution of 298 μM GLP-1 in
20 buffer was prepared, as described above. Final concentrations
21 of GLP-1 were 25, 50, 75, 100 and 150 μM , and the samples
22 were incubated with 50 μM ThT and 0.01 % NaN_3 (added to
23 prevent bacterial growth). 50 μM ThT was chosen as the ag-
24 gregation kinetics were shown to be independent of ThT con-
25 centration between 10-80 μM ThT, Fig. S1. 120 μL of the
26 peptide/ThT samples were pipetted into a 96-well half-area
27 plate made of black polystyrene with a clear bottom and a
28 non-binding surface (Corning 3881, USA). A sealing tape
29 (Costar Thermowell) was used to protect samples from evapo-
30 ration. Fluorescence measurements were carried out on a
31 Fluorostar Optima Microplate Reader (BMG Labtech, Offen-
32 burg, Germany), which was thermostatted at 37 $^{\circ}\text{C}$. ThT bind-
33 ing to fibrils was monitored by using an excitation filter at 440
34 nm and by recording the fluorescence emission at 480 nm.
35 Bottom reading of the plate every 30 min with 5 min of shak-
36 ing prior to each measurement was performed. Each cycle was
37 executed with the orbital shaker at 350 rpm, 5 flashes per well
38 and fluorescence measurements were made at a gain of 1000.

39 Each individual ThT datasets were fit to Equation 1,

$$40 \quad y=y_0 + A/(1 + \exp(-k(t-t_{1/2}))) + bt \quad (1)$$

41 where y_0 is the starting fluorescence, A the amplitude of the
42 transition, $t_{1/2}$ is the half-time, which is defined as the time at
43 which the ThT fluorescence has reached 50% of its final base-
44 line value, k is the apparent growth rate and b is the slope of
45 the final baseline. Note in many other studies, data are normal-
46 ized prior to fitting such that the inclusion of this additional
47 term is not needed. The lag time was calculated from the ki-
48 netic parameters obtained using Equation 2.^{15,20}

$$49 \quad t_{\text{lag}}=t_{1/2}-2/k \quad (2)$$

50 All measurements were made in triplicate for each peptide
51 concentration in a single 96-well plate, and each experiment
52 was repeated at least three times on different days with freshly
53 prepared samples.

54 **Analytical ultracentrifugation (AUC) sedimentation ve-
55 locity experiment.** Sedimentation velocity measurements
56 were performed at 20 $^{\circ}\text{C}$, 60,000 rpm using a Beckman Opti-
57 ma XL-I analysis ultracentrifuge equipped with an An-60Ti
58 rotor. The instrument was equipped with a UV-visible absorb-

59 ance detector. 150 μM GLP-1 was prepared in buffer and in-
60 cubated at room temperature for 2 hr before the start of the
experiment. 400 μL of the sample was loaded into the AUC
cell. The SEDFIT program was used to correct the sedimenta-
tion coefficient distributions to standard conditions and the
 $c(s)$ method was implemented.

www.analyticalultracentrifugation.com/default.htm

**Asymmetric flow field-flow fractionation with multi-
angle light scattering (AF4-MALS).** AF4-MALS was used to
separate and estimate the size of species in a 1500 μM solution
of freshly prepared GLP-1 sample in buffer using an Eclipse®
(Wyatt Technology Europe GmbH, Dernbach, Germany). The
AF4 was controlled by a high-performance liquid chromatog-
raphy system (HPLC, Agilent) equipped with UV/Vis and
MALS detectors (Wyatt Technology Europe GmbH, Dern-
bach, Germany). A 1 kDa cut-off polyether sulfone (PES)
membrane was used in the Eclipse SC channel for optimal
separation of species (Pall, New York, USA). Buffer was used
as the mobile phase and, the system was equilibrated overnight
prior to the experiment. The channel flow was maintained at 1
 mL min^{-1} and the cross-flow was varied: 4.5 mL min^{-1} from 0
to 2 min, 2.5 mL min^{-1} from 2 to 5 min, and 4.5 mL min^{-1} from
5 to 15 min, 4 mL min^{-1} from 15 to 20 min then 1 mL min^{-1}
from 20 to 30 min. Detection was accomplished using UV
absorbance at 280 nm and multi-angle light scattering. Data
from MALS were analysed by ASTRA (Wyatt Technology
Europe GmbH, Dernbach, Germany). The detectors were cali-
brated using BSA standards (Thermo Scientific). The calibra-
tion was validated by separation of 25 μL of 2 mg mL^{-1} BSA
in an appropriate mobile phase.

Dynamic Light Scattering (DLS). The intensity-weighted
mean hydrodynamic diameter distribution and the number size
distribution of freshly prepared GLP-1 (1500 μM) and fibrillar
GLP-1 (1500 μM) in buffer at room temperature (20 - 25 $^{\circ}\text{C}$)
were determined by DLS using a Zetasizer Nano ZS (Malvern
Instruments, Malvern, U.K.). A Zen 2112 cuvette and a scat-
tering angle of 173 $^{\circ}$ were used. The average values of the
polydispersity index (PDI) were obtained from the cumulants
analysis of the intensity autocorrelation function that was per-
formed by the Zetasizer Software provided by the manufactur-
er. Reported parameters were determined from an average of
at least three measurements.

Atomic force microscopy (AFM). GLP-1, either from (i) a
freshly prepared solution, or (ii) mature fibrils, were spread
onto freshly cleaved mica (SPI supplies, West Chester, PA).
The samples were then incubated for 20 min, followed by
washing with 200 μL of deionised water and dried under a
stream of nitrogen. Images were acquired in air at room tem-
perature (20-25 $^{\circ}\text{C}$) with a PicoPlus AFM instrument with a
PicoSPM II controller from Molecular Imaging (Agilent
Technologies, USA) in AC mode, equipped with a Miko-
Masch NSC26/No Al cantilever, between 65 and 130 Hz fre-
quency, force constant varying from 0.6 to 2.0 N m^{-1} (Innova-
tive Solutions Bulgaria Ltd., Sofia, Bulgaria). The images
were analysed with the open source software Gwyddion
(<http://gwyddion.net/>).¹⁶

61 RESULTS AND DISCUSSION

Aggregation kinetics. The aggregation kinetics of amyloid
fibril formation were measured starting from freshly prepared
samples of GLP-1 at three different pHs using ThT fluores-

cence. The aggregation was monitored over a range of peptide concentrations from 25 to 150 μM . Typical results are shown in Fig. 1. Kinetic parameters were determined by fitting the data to Eq. 1 and a lag time was then calculated for each dataset using Eq. 2. Standard sigmoidal curves were obtained for GLP-1 aggregation under all the conditions used, however, the kinetic parameters obtained from the fitting varied with pH and peptide concentration, Fig. 1. See SI2, Table S1 for further details.

At higher pH (≥ 8.2), the $t_{1/2}$ is found to decrease with increasing peptide concentration characteristic of a process following a nucleation-polymerization mechanism for fibril formation, Fig. 1F. Surprisingly at lower pH values there is either very little dependence on peptide concentration or the $t_{1/2}$ increases with increasing peptide concentration, Fig. 1D and B. These results were very reproducible. The highly unusual kinetics were observed for GLP-1 aggregation at pH 7.5 where the $t_{1/2}$ increases with increasing peptide concentration (the opposite of what is expected for a N-P model) suggesting other processes come into play, Fig. 1B. These unusual results have, to the best of our knowledge, been observed for just two other systems: ribosomal protein S6 (where a model involving an off-pathway oligomerization process was proposed)¹⁷ and immunoglobulin light chain (where an increase in concentration leads to a monotonic decrease in fibrillation propensity with an increasing protein concentration which has been related to dimer formation in the native state).¹⁸

In order to assess the degree to which GLP-1 monomer is converted into amyloid fibrils in the ThT assays, monomer depletion experiments were also undertaken, SI3. Using UPLC methods (ultra-pressure liquid chromatography), the loss in signal corresponding to monomeric, or small soluble oligomers of GLP-1 was monitored with time, Fig. S2. After 120 hr at pH 7.7 at 37 $^{\circ}\text{C}$, a solution of 75 μM GLP-1 was almost completely converted into high molecular weight species, Fig. S3.

Characterization of freshly prepared samples of GLP-1 in buffer, at the starting point of the kinetic assays, at different pH values. A wide range of biophysical techniques were used to fully characterize the structure and properties of freshly prepared samples of GLP-1 at pH 7.5, 8.0 and 8.5. The structure of species in solution was probed using far-UV CD, the hydrophobic surface area using ANS-binding assays, whilst the size of species in solution was investigated using SEC, AF4, AUC, DLS, AFM and TEM, see following sections

Characterization of the structure and hydrophobicity of freshly prepared GLP-1 samples. The far-UV CD spectra of freshly prepared samples of GLP-1 show that there is no change in the secondary structure with pH, Fig. S4. The average secondary structure is predicted to be approx. 30 % α -helix, 20% β -strand, 20% turns and 30% disordered between pH 7.5-8.5. ANS binding was also used to probe the exposed hydrophobic surface area.¹⁹ ANS binding to freshly prepared samples of GLP-1 at different pH values were assessed using fluorescence measurements over a range of peptide concentrations, see SI5 Fig. S5. The data clearly indicate that GLP-1 is more highly prone to form oligomers with exposed hydrophobic surface area at pH 7.5 relative to pH 8.0 or 8.5.

Characterization of the size distribution of species in freshly prepared GLP-1 samples. The size distribution of species in freshly prepared samples of GLP-1 was performed using a range of biophysical techniques from pH 7.5 to 8.5.

Although standard size-exclusion chromatography was useful to give an initial assessment of the size of the major species in solution for GLP-1 at different pH values (see SI6, Fig. S6), this method was unable to detect small populations of larger species. To do this, more sophisticated methods of analysis were required. Using AF4, we were successfully able to detect and separate monomeric GLP-1 from small oligomers present in the samples at both pH 8.0 and 8.5 (Fig. 2C and E). At pH 8.0 and 8.5, the distinct peaks observed likely correspond to a monomer and trimer with molecular weights of, 3.3 and 9.1 kDa at pH 8.0, and 3.3 and 11 kDa at pH 8.5, respectively. However, at pH 7.5, a single broad peak was observed suggesting a high level of heterogeneity of species in solution at this pH compared with the higher pHs, Fig. 2A. See SI7, Fig. S7 for further detail.

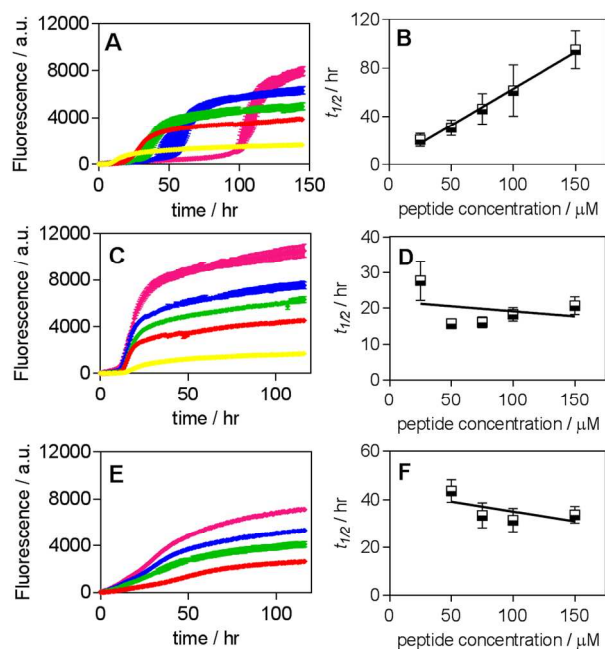


Figure 1. Aggregation kinetics of GLP-1 as a function of peptide concentration at different pHs. GLP-1 aggregation kinetics at pH 7.5 (A-B), pH 7.7 (C-D) and pH 8.2 (E-F). A, C, E show typical traces for the fibrillation of GLP-1 followed by ThT fluorescence at different GLP-1 concentrations. Each peptide concentration was run in triplicate. D, E and F show the dependence of the $t_{1/2}$ on the concentration of GLP-1. The error bars shown in A, C and E are the standard deviation from the mean for a single experiment in which each peptide concentration was run in triplicate. In B, D and F, the error bars correspond to the standard deviations of the kinetic parameters determined from three independent experiments each of which was run in triplicate.

Analytical centrifugation measurements of sedimentation velocities were also performed and, as with the AF4 data, similar velocity profiles were obtained at pH 8.0 and 8.5, (Fig. 2D & F). In these cases, the samples are mainly monomeric, however, small populations of both small and larger oligomers are present, Fig. 2D & F, insert figures and Table 1. Interestingly, the sedimentation velocity profile at pH 7.5 shows mainly monomer, Fig. 2B, however, the sample is much more polydisperse in comparison to the results at higher pH values. At pH 7.5, larger oligomers are not present, Table 1 and Fig. 2B. Molecular masses corresponding to a trimer determined using AUC were 12 kDa at pH 8.5 and 10 kDa at pH 8.0. At 7.5,

oligomeric species ranged from 6.9 to 12.6 kDa corresponding to a mix of dimer, trimer and tetramer, Fig. 2. See SI7, Fig. S7 for further detail.

Dynamic Light Scattering (DLS), a technique that is sensitive to large particles in solution, was also used to probe whether larger oligomeric species not detectable by AF4 or AUC, are present in solution. The DLS results (Fig. 3) confirmed that the main population has a small hydrodynamic radius that likely corresponds to GLP-1 monomer and the small oligomers detected by AF4 and AUC, Fig. 2. However, larger particles were also found to be present under all conditions, Fig. 3. These were also observed in both AFM and TEM images (see SI9, Fig. S9).

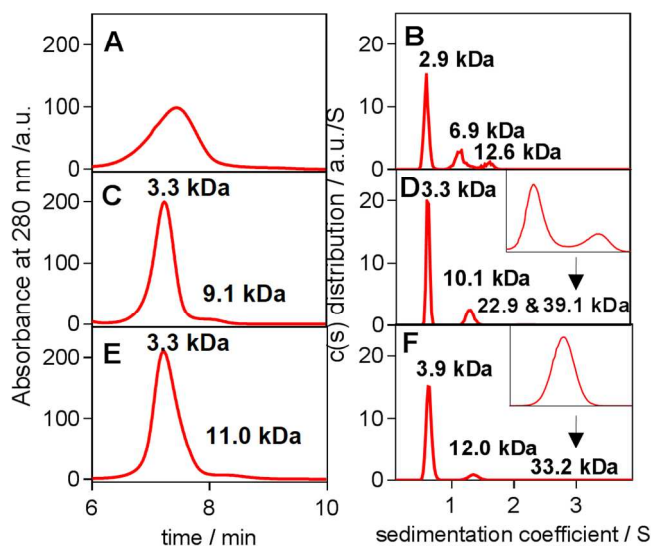


Figure 2. Size distribution of species in freshly prepared GLP-1 samples at different pHs determined using AF4 and AUC. (A-B) pH 7.5, (C-D) pH 8.0, and (E-F) pH 8.5. The left-hand column shows the AF4 results (A, C, and E) along with the M_w of monomers and small oligomers estimated using MALS (see Section SI7, Fig. S7 for more detail). The right-hand column shows the results of the AUC sedimentation velocity analysis of the GLP-1 samples illustrating the size distribution of sedimenting species obtained by $c(s)$ analysis.

Table 1. Percentage of oligomeric species present in freshly prepared GLP-1 samples.

| pH | Percentage of the species present, (%) | | |
|-----|--|-----------------|------------------|
| | Monomer | Small Oligomers | Larger Oligomers |
| 7.5 | 64 | 36 | not observed |
| 8.0 | 77 | 21.5 | 1.5 |
| 8.5 | 90 | 9.7 | 0.3 |

For more information see Section SI10 Table S4.

Fibril structure and morphology. The structure of the fibrils formed at the end of the ThT assays was investigated by far-UV CD, Fig. S4C. Although the spectra recorded at the three pH values are slightly different, they all show a broad minima around 218 nm characteristic of amyloid fibrils, Fig. S4C. AFM was also used to verify and characterise the fibrils formed under different conditions, Fig. 4. In these cases, 150 μ M GLP-1 samples at pH 7.5, 7.7, and 8.2 were allowed to aggregate at 37 $^{\circ}$ C for 200 hr in the presence of 50 μ M ThT and 0.01% NaN_3 . Fibrils were then retrieved and imaged using AFM, Fig. 4.

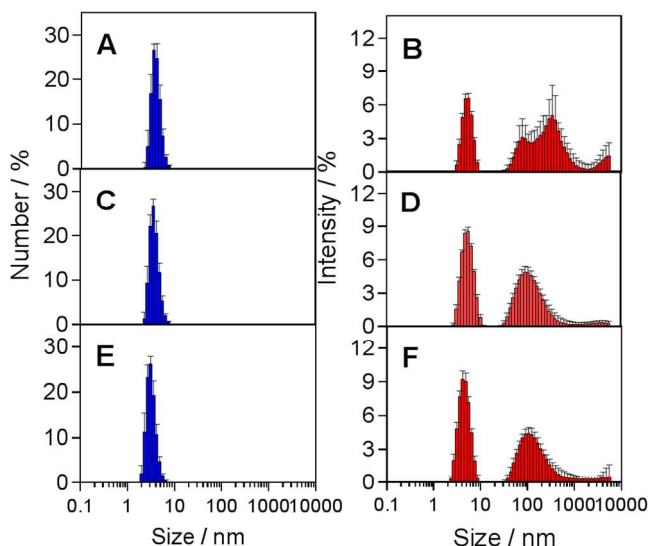


Figure 3. Dynamic Light Scattering results of freshly prepared GLP-1 at three different pHs. (A-B) pH 7.5, (C-D) pH 8.0, and (E-F) pH 8.5. The left-hand column shows the size distribution by number (A, C and E) and the right-hand column shows the size distribution by intensity (B, D and F). See Section SI8, Fig. S8 for more detail.

Fibrils formed at 37 $^{\circ}$ C, pH 7.7 and 8.2 are stable and typically 1 – 3 μ m in length and 10 - 15 nm in height and have a twist (Fig. 4 and SI11, Fig. S10). In contrast, the fibrils formed at pH 7.5 are short, thin, sticky and considerably more heterogeneous, Fig. 4. In addition, at pH 7.5, fibrils are unstable and dissociate after dilution (100 fold) either in water or buffer, Fig. 4B (see SI11, Fig. S10 for more detail). After dilution spherical-like morphologies are observed with diameters ranging from 0.1-0.4 μ m and heights ranging between 10 – 60 nm, Fig. 4B.

A model for GLP-1 aggregation under different conditions. The concentration of peptide^{20,21} and the presence of on-pathway oligomers²², are both known to be important in the formation of amyloid fibrils. Increasing peptide concentration usually leads to an increase in the rate of fibrillation as observed by a reduction in lag time^{6,20}, a feature that is typical of a nucleation-polymerization mechanism²⁰. For GLP-1 at pH values over 8.0 an inverse relationship between lag time and peptide concentration is observed and, in this case, a simple nucleation-polymerization mechanism can be proposed where monomer (M) first associates into oligomers (O_m) that are on-

pathway to fibril formation, Fig. 5. For GLP-1, under these conditions, this is a slow nucleated process which leads to the specific formation of stable fibrils, which are long, stable and twisted, Fig. 4.

However, the simple nucleation-polymerization model does not explain the unusual kinetic data obtained at pH 7.5. Under these conditions, we propose a more complex model in which there is competition between the formation of on-pathway

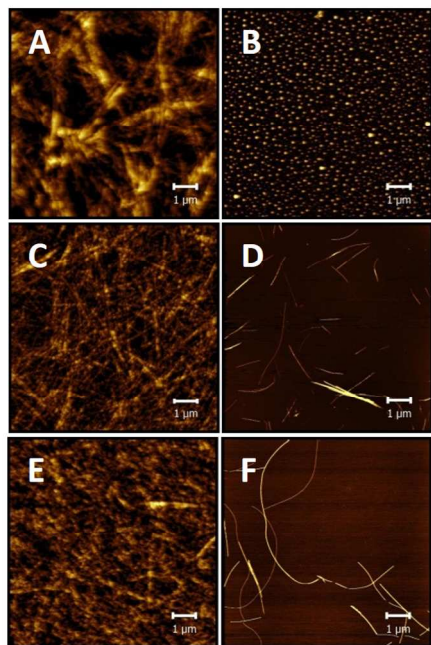


Figure 4. Atomic force microscopy images of typical GLP-1 fibrils formed under different conditions. (A-B) pH 7.5, (C-D) pH 8.0, and (E-F) pH 8.5. The left-hand column shows AFM images of samples of 150 μM GLP-1 aggregated for 200 hr at 37 $^{\circ}\text{C}$. The right-hand column shows AFM images of the fibrils diluted 100 times into deionized water prior to imaging (see Section S11 Fig. S10 for more details).

oligomers leading to fibrils, and the formation of a different form of oligomer, which has to be off-pathway, Fig. 5. Powers and Powers have elegantly modeled such a mechanism mathematically²³. They have shown that, under specific kinetic conditions where a set of assumptions can be applied, that a positive slope is obtained for a plot of $t_{1/2}$ versus the concentration of monomer.²³ They propose that this is an essential piece of evidence consistent with their off-pathway model.²³ This is what we observe for GLP-1 at pH 7.5, Fig. 1B.

We are not the first to observe such dependence experimentally and propose a kinetic scheme in which off-pathway as well as on-pathway oligomeric species form. This has also been observed in the fibrillation of immunoglobulin light chain L_{EN}¹⁸ and S6 ribosomal protein¹⁷. In both these cases, the polypeptide starts as a globular folded protein rather than a relatively unstructured and dynamic short peptide such as GLP-1. Here, we present strong evidence that off-pathway oligomers are also populated during the fibrillation of GLP-1 at pH 7.5, highlighting this as a more general phenomenon and putting the concept proposed some years ago on firm experimental ground.

Kinetic modeling of on- and off-pathway oligomer models.

In order to verify that an off-pathway species would give rise

to the difference in aggregation kinetics observed, three models for the fibrillation of GLP-1 were created within the program KinTek (see S112 for further details). In the first model (Model 1), we used a simple model of nucleation-polymerization and demonstrated that the kinetic parameter $t_{1/2}$ decreases with increasing peptide concentration as expected, Fig. S11A, C. We then added an off-pathway reaction where monomer converts through monomer addition to create a series of off-pathway oligomers and added this to our starting nucleation-polymerization model to generate Model 2. This model also shows a decrease in $t_{1/2}$ with increasing peptide concentration, Fig. S11B, D. However, addition of the off-pathway oligomers to the reaction scheme in Model 1, resulted in a delay in $t_{1/2}$ as shown in Fig. S11E-F, which show the amount of fibril formation (in terms of monomer concentration) with time at 25 and 150 μM monomer starting concentrations. $t_{1/2}$ increased on addition of the off-pathway species, from 53 to 94 hr at 25 μM , and from 8.6 to 16 hr at 150 μM monomer. These results confirm that the presence of off-pathway species results in an increase in the length of time it takes for sufficient nuclei to be formed, however, Model 2 does not fully explain the results obtained for GLP-1. A third model, Model 3, was created which was essentially the same as Model 2 except an additional unimolecular step was included where monomers M interconvert with a different form of monomer, M^* , and only M^* forms the on-pathway oligomers required for fibril formation. In this case, the dependence of the $t_{1/2}$ on initial monomer concentration switches such that it increases with increasing starting concentration, Fig. S11H, as we observe experimentally for GLP-1 at pH 7.5.

Thus, our results on GLP-1 at pH 7.5 are consistent with the presence of off-pathway oligomeric species, as well as, a unimolecular step on-pathway to fibril formation.

Studies on rat and human isoforms of the amyloidogenic protein IAPP, associated with diabetes in humans, have recently established that various oligomeric species can be found under conditions where human IAPP forms amyloid fibrils.²⁴ In this case, a detailed analysis of the structure and properties of the different oligomers revealed that only the globally flexible, low-order oligomers, which did not bind ANS nor have extensive β -sheet secondary structure, were toxic to cells.²⁴ These results raise the interesting question of whether the on- and off-pathway oligomers that we have shown form at different pH values for GLP-1 may also have different properties including potentially different cell toxicity.

Origin of the pH-induced switch in mechanism for GLP-1 aggregation.

Net charge on the peptide in its monomeric state. It is well established that the total charge on a peptide or protein can play an important role in determining its propensity towards aggregation.²⁵⁻²⁶ Normally, the closer the net charge is to zero the higher propensity to aggregate, as there is little or no unfavorable electrostatic interactions to overcome to form oligomeric species and nuclei.²⁵

In order to better understand our results, we used PropKa in the Schrodinger Suite to calculate the pK_a values and therefore the charge on each ionizable group in GLP-1 as a function of pH, S113. Two structures were used as starting points: 1D0R, which is an ensemble of structures calculated from NMR experiments performed in trifluoroethanol (TFE), Fig. S12A &

1 B, and 3IOL, the structure of GLP-1 bound to its receptor. In
 2 both cases, GLP-1 is highly helical with more residues in-
 3 volved in α -helix formation than our far-UV CD data in aque-
 4 ous buffer suggest, Fig. S4. However, as no unbound structure
 5 for GLP-1 in water is available, these structures were used.
 6 Both structures gave very similar results, SI13, Figures S12 &
 7 S13. The charge on each ionisable group and the overall net
 8 charge on the peptide are shown in Fig. S12C and D, respec-
 9 tively. The results show that there are two ionisable groups
 10 that change ionization state between pH 7.5 and 8.5: the N-
 11 terminus and the side chain of His1. The pK_a of His1 < 7
 12 whilst that of the N-terminus is approx. 8. The pK_a of the N-
 13 terminus is affected by the fact that it can form hydrogen
 14 bonds with backbone amide groups as observed in the ensem-
 15 ble of structures generated from the NMR data, Fig. S12B. On
 16 the basis of these results, we propose that the protonation state
 17 of the N-terminus plays a critical role in the formation of off-
 18 pathway oligomers. When positively charged, i.e., at pH val-
 19 ues below its pK_a of approx. 8, then off-pathway oligomers are
 20 favoured over on-pathway oligomers. In contrast, at pH val-
 21 ues above its pK_a , when it is uncharged, on-pathway oligomers
 22 are favoured. Thus, analogs of GLP-1 that are N-terminally
 23 acetylated may well not show this unusual behavior.

24 Do the aggregation kinetics of GLP-1 follow the general rule
 25 that aggregation propensity increases the lower the net charge
 26 on the peptide?²⁵⁻²⁶ The pK_a calculations suggest that GLP-1
 27 has no overall net charge at approx. pH 5.5, Fig. S12D and
 28 S13B. However, aggregation kinetics cannot be measured at
 29 this pH due to solubility problems. The net charge is predicted
 30 to increase between pH 7.5 and 8.5 due to the deprotonation of
 31 the N-terminus (from an overall net charge of approx. -1/-2 to
 32 -2/-3, Fig. S12D and S13B). Experimentally, we observe an
 33 increase in the propensity of GLP-1 to form fibrils, counter to
 34 what might be expected. However, one can argue that there is
 35 an increase in the aggregation propensity of GLP-1 as its over-
 36 all charge reduces, i.e., moving towards pH 5.5, but that it is
 37 an increased tendency to form off-pathway oligomers not on-
 38 pathway oligomers that would lead to amyloid fibril forma-
 39 tion. In this regard, it is important to define specifically the
 40 aggregation state, as many such states – on- and off-pathway
 41 oligomers, fibrils etc. may exist.

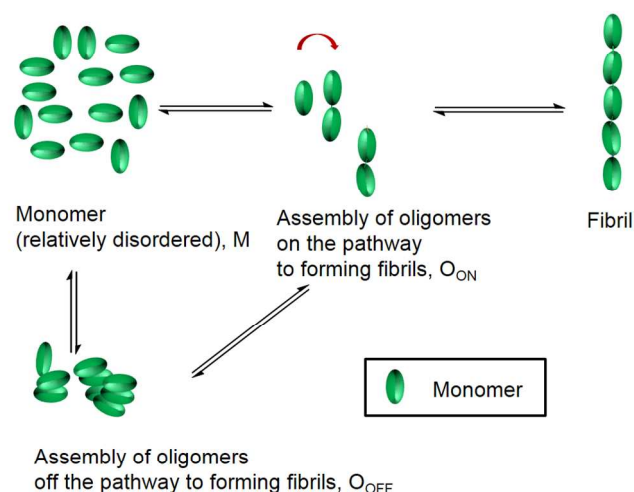


Figure 5. Proposed mechanism for GLP-1 fibril formation.

There are two pathways, one in which the monomer (M) associates to form on-pathway oligomers (O_{ON}) which can convert directly into fibrils. On the second pathway, monomers can form a different oligomeric state (O_{OFF}) which is not on the direct pathway to fibril formation. The on- and off-pathway oligomers may be able to interconvert, however, the energy barriers to interconversion are likely high and the kinetics slow.

Net charge on the peptide in the oligomers. The discussion above relates to the net charge and pK_a values of ionisable groups in a highly helical, monomeric form of GLP-1. We cannot rule out that it is not the net charge of the monomer that is important, but the net charge and pK_a values of ionisable groups in the different oligomeric species that play the dominant role in the pH effects observed. Our results suggest that differences in the size and structure of the on- and off-pathway oligomers may lead to different responses to changes in pH over the range studied. In particular, the stability or the kinetics of formation/dissociation of the two oligomeric species may have different pH dependencies.

CONCLUSIONS

In conclusion, we have presented unusual aggregation kinetic data for GLP-1 at pH 7.5, where the lag time increases with increasing peptide concentration. These results indicate the likely existence of off-pathway oligomeric species which we believe form rapidly relative to the on-pathway oligomers, and which therefore act as a sink of monomers. These off-pathway oligomers will slowly dissociate and can, therefore in time, form on-pathway oligomers and ultimately fibrils. However, in addition there has to be an initial unimolecular conversion of the monomer to a different monomeric species which can form on-pathway oligomers and ultimately fibrils. These monomers at pH 7.5, the fibrils formed by GLP-1 are short and unstable. At slightly higher pH values, $pH \geq 8.2$, the aggregation kinetics of GLP-1 revert back to the simple and

frequently observed, nucleation-polymerization mechanism where only on-pathway oligomers are formed to any extent.

Using a number of biophysical techniques, we were successfully able to detect a range of small oligomers present in GLP-1 samples at all the pH values studied, establishing that monomeric GLP-1 is in equilibrium with either a dimer and/or a trimer, as well as and other slightly larger oligomeric species even in freshly prepared samples of very pure peptide. The results demonstrate that, at pH 7.5, GLP-1 has a higher propensity to form oligomeric species, consistent with our proposed mechanism under these conditions where there is a rapid and non-specific aggregation of GLP-1 into oligomers which are off-pathway.

It is also of interest to note that, under conditions where GLP-1 is very prone to forming oligomers (pH 7.5), the fibrils it forms under these conditions are short and relatively unstable. In contrast, increasing the pH by as little as 0.5 has a dramatic effect. Slightly higher pH values, where the monomeric form is more stable and therefore small oligomers much less prevalent at the beginning of the reaction, favors the formation of on-pathway oligomers and ultimately the formation of much more stable fibrils which are long and twisted.

ASSOCIATED CONTENT

Supporting Information. Supplementary results on the design and control of experiments to confirm the presence of small oligomers in freshly prepared samples of GLP-1, together with detailed aggregation kinetic data. Experimental procedures for AFM imaging and the determination of fibril morphology. Supplementary Figures and Tables described in the paper. This material is available free of charge via the Internet at <http://pubs.acs.org>.

AUTHOR INFORMATION

Corresponding Author

*sej13@cam.ac.uk

Author Contributions

The experimental programme of research was planned by KLZ, ADS and SEJ, and performed by KLZ. SEJ and FJB undertook the Kintek modeling. The manuscript was written by KLZ, ADS and SEJ. All other authors contributed to general discussions. All authors have given approval to the final version of the manuscript.

Funding Sources

The research was funded by MedImmune, and was carried out in the Chemistry Department and the Nanoscience Centre at the University of Cambridge, UK and MedImmune, Granta Park, Cambridge, UK.

ACKNOWLEDGMENT

The authors would like to acknowledge Dr. Myriam Ouberai (University of Cambridge, U.K.) for her help with AFM measurements, and Dr. Katherine Stott (University of Cambridge, U.K.) for her assistance in using analytical ultracentrifugation. We thank Dr. Adrian Podmore and Dr. Raphael J. Gubeli from MedImmune Ltd. for help with setting up the AF4 experiment. Dr. Alexander K. Buell and Georg Meisl are also acknowledged for helpful discussion (both from University of Cambridge). We would also like to acknowledge Davide Branduardi who performed the pK_a calculations, and Eric Feyant and Andrew Sparkes for interesting discussions (Schrödinger). This work was supported by MedImmune Ltd.

ABBREVIATIONS

AFM, atomic force microscopy; AUC, analytical ultracentrifugation; TEM, transmission electron microscopy; AF4, asymmetric flow field-flow fractionation; ThT, thioflavin T; CD, circular dichroism; DLS, dynamic light scattering; MALS, multi-angle light scattering.

REFERENCES

- (1) Frokjaer, S.; Otzen, D. E. *Nature reviews. Drug discovery* **2005**, *4* (4), 298.
- (2) Greenwald, J.; Riek, R. *Structure (London, England : 1993)* **2010**, *18* (10), 1244.
- (3) Tycko, R.; Wickner, R. B. *Accounts of Chemical Research* **2013**, *46* (7), 1487.
- (4) Eichner, T.; Radford, S. E. *Molecular Cell* **2011**, *43* (1), 8.
- (5) Arosio, P.; Knowles, T. P. J.; Linse, S. *Phys. Chem. Chem. Phys.* **2015**, *17*, 7606.
- (6) Cohen, S. I. A.; Vendruscolo, M.; Dobson, C. M.; Knowles, T. P. J. *Journal of molecular biology* **2012**.
- (7) Chiti, F.; Dobson, C. M. *Annual Review of Biochemistry* **2006**, *75* (1), 333.
- (8) Fändrich, M. *Journal of molecular biology* **2012**, *421* (4–5), 427.
- (9) Buell, A. K.; Galvagnion, C.; Gaspar, R.; Sparr, E.; Vendruscolo, M.; Knowles, T. P. J.; Linse, S.; Dobson, C. M. *Proceedings of the National Academy of Sciences of the United States of America* **2014**, *111* (21), 7671.
- (10) Buell, A. K.; Dobson, C. M.; Knowles, T. P. J. *Essays in biochemistry* **2014**, *56* (1), 11.
- (11) Drucker, D. J. *Nature clinical practice. Endocrinology & metabolism* **2005**, *1* (1), 22.
- (12) Drucker, D. J. *Diabetes* **2015**, *64* (2), 317.
- (13) Poon, S.; Birkett, N. R.; Fowler, S. B.; Luisi, B. F.; Dobson, C. M.; Zurdo, J. *Protein and peptide letters* **2009**, *16* (12), 1548.
- (14) Jha, N. N.; Anoop, A.; Ranganathan, S.; Mohite, G. M.; Padinhateeri, R.; Maji, S. K. *Biochemistry* **2013**, *52* (49), 8800.
- (15) Alvarez-Martinez, M. T.; Fontes, P.; Zomosa-Signoret, V.; Arnaud, J. D.; Hingant, E.; Pujo-Menjouet, L.; Liautard, J. P. *Biochimica et Biophysica Acta - Proteins and Proteomics* **2011**, *1814* (10), 1305.
- (16) Nečas, D.; Klapetek, P. *Open Physics* **2012**, *10* (1), 181.
- (17) Deva, T.; Lorenzen, N.; Vad, B. S.; Petersen, S. V.; Thørgersen, I.; Enghild, J. J.; Kristensen, T.; Otzen, D. E. *Biochimica et biophysica acta* **2013**, *1834* (3), 677.
- (18) Souillac, P. O.; Uversky, V. N.; Fink, A. L. *Biochemistry* **2003**, *42* (26), 8094.
- (19) Lindgren, M.; Sörgjerd, K.; Hammarström, P. *Biophysical journal* **2005**, *88* (6), 4200.
- (20) Nielsen, L.; Khurana, R.; Coats, A.; Frokjaer, S.; Brange, J.; Vyas, S.; Uversky, V. N.; Fink, A. L. *Biochemistry* **2001**, *40* (20), 6036.
- (21) Powers, E. T.; Powers, D. L. *Biophysical journal* **2006**, *91* (1), 122.
- (22) Lorenzen, N.; Nielsen, S. B.; Buell, A. K.; Kaspersen, J. D.; Arosio, P.; Vad, B. S.; Paslawski, W.; Christiansen, G.; Valnickova-Hansen, Z.; Andreasen, M.; Enghild, J. J.;

- 1 Pedersen, J. S.; Dobson, C. M.; Knowles, T. P. J.; Otzen, D.
2 E. *Journal of the American Chemical Society* **2014**, *136*
3 (10), 3859.
- 4 (23) Powers, E. T.; Powers, D. L. *Biophysical journal* **2008**, *94*
5 (2), 379.
- 6 (24) Abedini, A.; Plesner, A.; Cao, P.; Ridgway, Z.; Zhang, J.;
7 Tu, L.-H.; Middleton, C. T.; Chao, B.; Sartori, D.; Meng, F.;
8 Wang, H.; Wong, A. G.; Zanni, M. T.; Verchere, C. B.;
9
10
11
12
13
14
15
16
17
18
19
20
21
22
23
24
25
26
27
28
29
30
31
32
33
34
35
36
37
38
39
40
41
42
43
44
45
46
47
48
49
50
51
52
53
54
55
56
57
58
59
60
- Raleigh, D. P.; Schmidt, A. M. *eLife* **2016**, *5*, 1.
- (25) Chiti, F. In *Protein misfolding, aggregation and conformational diseases: Part A: Protein Aggregation and Conformational Diseases*; Vladimir Uversky, A. F., Ed.; Springer: New York, 2007; pp 47–50.
- (26) Roberts, C. J. *Trends in Biotechnology* **2014**, *32* (7), 372.